Proc. 18th Winter Workshop on
Nuclear Dynamics (2002) 000–000

18th Winter Workshop
on Nuclear Dynamics
Nassau, Bahamas
January 20–27, 2002

Particle Correlations with the PHENIX Experiment

Stephen C. Johnson

Physics and Advanced Technologies Directorate
Lawrence Livermore National Lab
Livermore, CA 94550

Abstract. Results of identical pion correlations from the first year of data collection with the PHENIX detector at RHIC ($\sqrt{s_{NN}}$=130GeV) are presented. PHENIX has good particle identification using an electromagnetic calorimeter for timing, leading to identified pions from .2 to 1 GeV/c. This extends the range of previously measured correlation radii at this energy to $\langle k_T \rangle$=633MeV/c. The beam energy dependence of the HBT radii are studied in depth and no significant dependence of the transverse radii is present. The longitudinal correlation length has a moderate energy dependence. Furthermore, theoretical predictions of R_{out}/R_{side} severely underpredict the measured ratio, which is consistent with unity for all k_T. The implications of these results are considered.

Keywords:
PACS:

1. Theoretical Considerations

1.1. The Physics of GGLP

A distortion of the two particle probability distribution by the influence of Bose-Einstein statistics was first noted by the quartet of physicists Goldhaber, Goldhaber, Lee, and Pais in $p\overline{p}$ collisions in 1960 [1]. This observable was subsequently adopted in a variety of systems as a technique to probe the space-time history of the collision region. For a recent review see [2].

The normalized two particle probability distribution, $P(p_1, p_2)/P(p_1)P(p_2)$, is given by the ratio of the two particle probability distribution to the square of the single particle distributions. This function is defined as the ‘correlation function’ and, for a static source with no final state interactions, is related to a Fourier transform of the source spatial distribution ($\rho(r)$) with respect to the momentum difference, q , $C_2 \approx 1 + \tilde{\rho}(q)^2$. A more general expression for the correlation function is:

ISBN 963 00 0000 0

$$C(\vec{q},\vec{k}) = 1 + \frac{|\int d^4xS(x,p)e^{iq\cdot x}|^2}{|\int d^4xS(x,p)|^2} \tag{1}$$

Due to experimental statistical limits, it has to date been practically impossible to study the full six dimensional correlation function. Instead, in most cases we take advantage of the event averaged impact parameter to reduce our nominally azimuthally asymmetric source into a symmetric one [1]: $(\vec{q},\vec{k}) \rightarrow (\vec{q},k_T,y)$. Historically, experimentalists have plotted $C_2(\vec{q})$ while cutting on k_T and y.

1.2. A Note on Frames

The appropriate choice of reference frame for the correlation function depends on our physical assumptions of the source. Traditionally experimentalists and theorists in relativistic heavy ion collisions have chosen the longitudinally comoving system (LCMS) as the appropriate frame and deconvolute $\vec{q}$ into components long, side and out. The 'long' component is the along the beam direction; the 'out' component is in the direction of the average transverse momentum of the pair; and the 'side' component is the complementary orthogonal component perpendicular to the transverse motion of the pair. This choice of frame assumes a longitudinally boost invariant source and has the very nice feature that a static long lived source results in $R_{out} \gg R_{side}$. This feature is significant in searches for a quark gluon plasma where a phase transition is accompanied by a large latent heat and long lived source.

However, if the source is expanding, the LCMS parametrization sees a Lorentz contracted outwards radius, not the true coherence length of the source in its rest frame (R_{out}^{TRUE}). As such, measurements of the HBT radii are distorted not only by the fact that we measure only "lengths of homogeneity" but also by Lorentz boosts of the source in the outwards direction. We can place some boundaries on the actual size of the outwards radius by noting that the largest value of R_{out} is measured in the pair center of mass frame (PCMS). All other frames related to the PCMS frame by a boost in the direction of the transverse momentum have a smaller measured outwards radius, $R_{out}^{PCMS}/\gamma_{pr}$, where γ_{pr} is the gamma boost from the PCMS to the measured frame. A lower limit can also be placed on the true out radius if we are willing to assume that the source is not moving faster than the PCMS frame and is not going backwards: $R_{out}^{TRUE} \geq R_{out}^{LCMS}$.

Consider a simple example of a source moving at $\beta_s = 0.7$ towards the detector while emitting pairs with mean average momentum of $\langle k_T \rangle = 300$ MeV. In this case, if the outwards radius measured in the LCMS frame is $R_{out}^{LCMS} = 5$ fm, then the radius measured in the PCMS is simply $\gamma_{pr} R_{out}^{LCMS} = 11.8$ fm. However, the true source in its rest frame has a radius of $\sqrt{\frac{1}{1-\beta_s}} R_{out}^{LCMS}$ =7 fm.

[1] see [3] for a very interesting counter example.

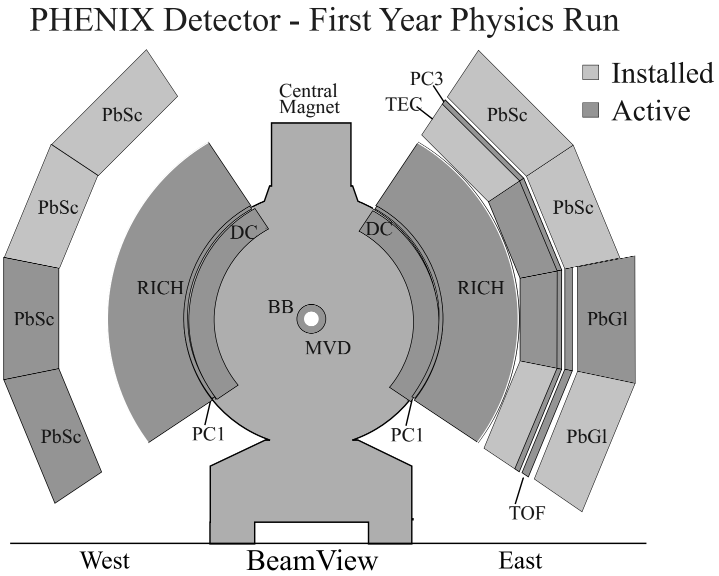

Fig. 1. The PHENIX experimental configuration in the first year of data taking.

2. Experimental Measures

2.1. The PHENIX Experiment

The PHENIX experiment has been described in detail elsewhere [5]. It is composed of 4 "arms": two arms perpendicular to the beam specializing in electron, photon and hadron identification ("central arms") and two arms for measuring muons ("muon arms"). A beams-eye view of the central arms is shown in Figure 1.

The central arms, covering a psuedo-rapidity region $|\eta| < 0.35$, are composed of a variety of subdetectors used in concert for particle identification and momentum determination. For the analysis in this note, we use detectors only on the west arms. The beam-beam counters (BBC) and zero degree calorimeters (ZDC) were used to trigger on inelastic interactions and determine the centrality of the collision; the drift chamber (DC), and pad chamber (PC) are used for three dimensional pattern recognition and momentum determination; the association of the track with a cluster in the electromagnetic calorimeter (EMC) in conjuction with the BBC start time determines the velocity of the particle.

2.2. Analysis Details

Centrality is defined by the measured zero degree neutral energy in the ZDC and the produced particle multiplicity measured in the BBC [6]. For this analysis we consider events in the 30% most central range of the inelastic cross section. The mean centrality of all pairs in this sample is 10%. In the first year data sample this corresponds to 493K events after all offline cuts.

The mass of particles is determined in the anlysis through a combination of momentum and velocity information. Momentum dependent bands are both measured experimentally and determined analytically from the momentum resolution of the DC and PC ($\delta p/p = 0.6 \oplus 3.6\% p$) and timing resolution of the EMC-BBC pair (600 ps). Pions are defined as being within 1.5σ of the pion mass peak and at least 2.5σ from the kaon peak. The resulting dataset contains 3.1 million π^+ pairs and 3.3 million π^- pairs. The mixed background is constructed from the pair dataset through the random choice of two pions from pairs in different events. Due to the changing detector acceptance as a function of collision position we require that all mixed pairs come from events with a reconstructed BBC collision vertex within 1cm of each other.

To further minimize the influence of detector induced artifacts in the correlation function we introduce a number of cuts on both the real and mixed pair distributions. We require that all pairs are at least 2cm from each other in the drift chamber to suppress close-track inefficencies and ghosts. Pairs that share the same EMC cluster are also removed from both the real and mixed samples.

The correlation function is created by forming the ratio of real to mixed pairs versus the momentum difference of the pair. This raw correlation function is further corrected for the known Coulomb interaction of the pions of the pair with one another. The correction is performed by making the simplifying assumption of a Gaussian source in the pair center of mass frame and using an iterative proceedure [7]. The extracted radii have been studied as a function of both the radius ($R_{Coulomb}$) of the source and the strength of the coulomb interaction ($\Lambda_{Coulomb}$) and are found to vary by no more than .25 fm in any dimension versus reasonable variations of $R_{Coulomb}$ ($\pm 20\%$) and $\Lambda_{Coulomb}$ ($.5 \to 1.0$). The results quoted below use the nominal extracted radius ($R_{Coulomb} = R_{inv}$) and full Coulomb correction ($\Lambda_{Coulomb} = 1.0$).

Finally, the correlation function is fit using a log-likelihood MINUIT based minimization method to the functional form

$$C_2 = 1 + \lambda \prod_{i=x,y...} exp(-R_i{}^2 q_i{}^2)$$

where i= inv for the one dimensional fit, i = long, side, out for the LCMS fit, etc.

2.3. Results

A projection of the π^- three dimensional correlation function is shown in Fig. 2 with its corresponding fit. This particular plot includes the entire unbinned dataset.

The k_T dependence of the correlation function provides extra information on the dynamics of the source so we divide our results into three bins in k_T from 200-400 MeV, 400-550 MeV and 550-1000 MeV. The corresponding $\langle k_T \rangle$ are 333 MeB, 472 MeV and 633 MeV, respectively. In each k_T bin we determine R_{inv}, as well as three dimensional fits in the LCMS and PCMS frame. The results are shown in Table 1.

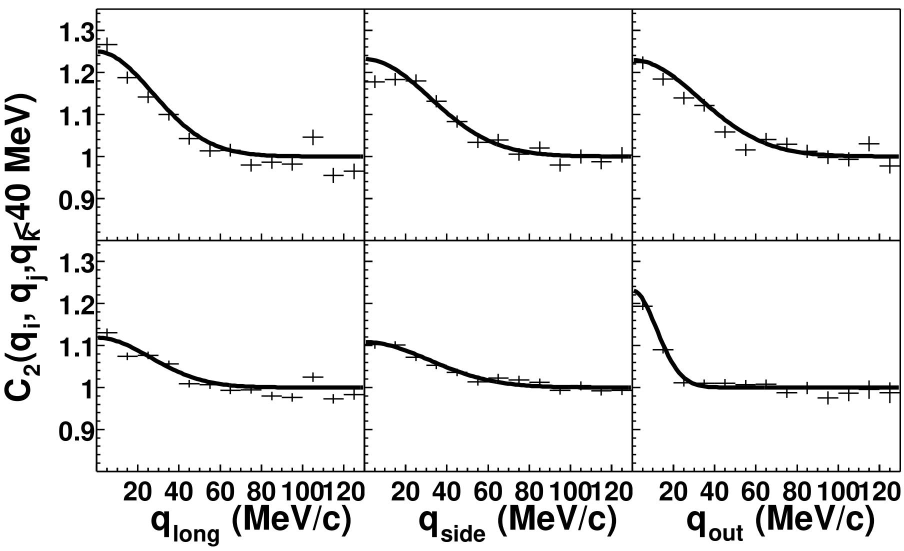

Fig. 2. The three dimensional correlation function for π^- pairs versus q_{long}, q_{side}, and q_{out} in both the LCMS frame (top) and pair center-of-mass frame (bottom). The data are plotted versus one momentum difference variable while requiring the other two to be less than 40 MeV/c. The lines correspond to the fit to the entire distribution.

Table 1. The k_T dependencies of the π^+ and π^- radii in the LCMS and PCMS frames. All momenta are in MeV and all radii are in fm. The errors are statistical only.

	k_T (MeV)	$200-400$	$400-550$	$550-1000$
	$\langle k_T \rangle$	333	472	633
π^+	R_{inv}	6.74 ± 0.31	6.42 ± 0.46	3.46 ± 0.46
	λ_{LCMS}	0.423 ± 0.037	0.389 ± 0.039	0.287 ± 0.048
	R_{long}	6.01 ± 0.45	4.76 ± 0.35	2.97 ± 0.38
	R_{side}	4.81 ± 0.30	3.74 ± 0.36	2.79 ± 0.37
	R_{out}	4.78 ± 0.30	3.76 ± 0.26	2.59 ± 0.46
	R_{out}^{PCMS}	11.35 ± 0.69	12.20 ± 1.02	8.60 ± 1.13
π^-	R_{inv}	6.00 ± 0.30	5.96 ± 0.41	4.58 ± 0.48
	λ_{LCMS}	0.431 ± 0.079	0.405 ± 0.067	0.353 ± 0.062
	R_{long}	5.69 ± 0.76	4.77 ± 0.49	3.76 ± 0.41
	R_{side}	4.67 ± 0.38	4.13 ± 0.45	3.22 ± 0.35
	R_{out}	4.69 ± 0.58	3.75 ± 0.40	2.81 ± 0.34
	R_{out}^{PCMS}	11.27 ± 0.72	12.42 ± 1.18	11.89 ± 1.73

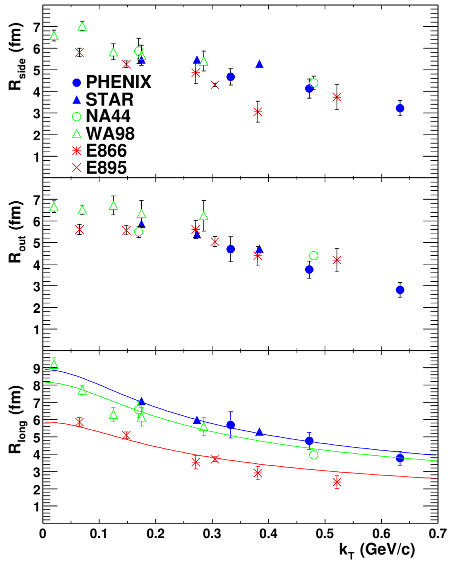

Fig. 3. The k_T dependence of published radii in the LCMS frame for various beam energies and experiments near mid-rapidity. RHIC measurements at $\sqrt{s_{NN}}$ = 130GeV/c are in blue; SPS measurements at $\sqrt{s_{NN}}$ = 17.3GeV/c are in green; AGS results at $\sqrt{s_{NN}}$ = 4.9 and 4.1 GeV/c are in red. The lines are a fit to $1/\sqrt{m_T}$ to all results (π^+ and π^-) for a given beam energy. The data are for π^- pairs except for the NA44 results, which are for π^+.

3. Interpretation

The recent correlation results measured at RHIC, both by PHENIX [14] and STAR [15] have generated a great deal of interest and confusion in the theoretical community [16]. Much of the non perturbative measurements at RHIC in the first year of data taking can be well described in the context of a hydrodynamic model. However, the correlation results have strained the parameters of these models to unphysical values, prompting a theoretical reevaluation.

3.1. Comparisons

Figure 3 places the measurements by PHENIX in the context of those at other energies and by other experiments [15, 8, 9, 12, 13].[2] As is clear, the $k_T$dependence of all three LCMS radii are very similar over a wide range of beam energies ($\sqrt{s_{NN}}$ = 4.1 to 130 GeV/c). Indeed the transverse radii are nearly identical over the entire energy range. The only clear energy dependence is in the longitudinal component which increases moderately as a function of energy.

To quantify the differences in R_{long} as a function of beam energy, we fit each k_T dependence to a hydrodynamically inspired equation [10, 11] [3] : $R_{long} = A/\sqrt{m_T}$. The results, overlayed with the data in Fig. 3, are $A = 3.32 \pm 0.03$, 2.9 ± 0.1 and 2.19 ± 0.05 fm·GeV$^{\frac{1}{2}}$ for $\sqrt{s_{NN}}$=130, 17.3 and 4.9/4.1 GeV, respectively.

[2] We plot the $\sqrt{s_{NN}}$=4.9 [12] and $\sqrt{s_{NN}}$=4.1 [13] together due to their minimal energy difference.

[3] This functional form is supported by a theoretical approximation to first order of R_{long}versus T/m_T. In this form, $A = \tau_0 T$ where τ_0 is the proper hadronization time.

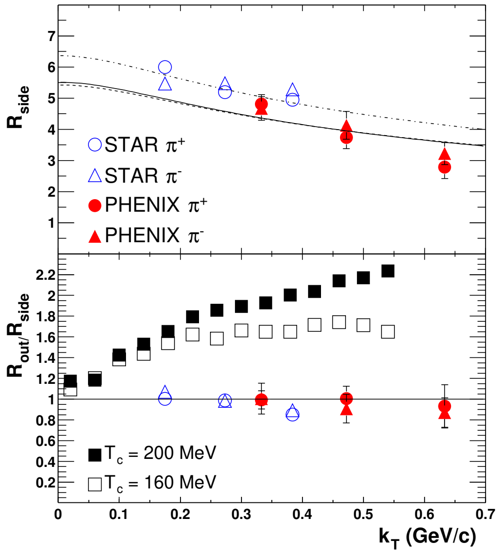

Fig. 4. The top panel shows the measured $R_{side}$from identical pions for both STAR and PHENIX. The solid line is a fit of Eq. 3 to the PHENIX data, and the dashed line is the same fit for Eq. 2. The dot-dashed line is a fit of Eq. 3 to the STAR data. The bottom panel shows the ratio R_{out}/R_{side}as a function of $k_T$overlayed with theoretical predictions for a phase transition for two critical temperatures.

There are at least two outstanding issues that have avoided easy physical descriptions: (1) the absolute magnitude of the radii and their shape in k_T at RHIC is stikingly similar to lower energy measurements even though the particle multiplicity per unit rapidity increases by a factor of three over the same energy range; (2) the ratio of the transverse radii R_{out}/R_{side} is equal to 1 over all k_T.

The first puzzle, that of small radii, has been most troubling in the description of R_{long} which has been irreproduceable in hydrodynamic calculations, with predictions 20-50% higher than the data [16].

The second puzzle, regarding the R_{out}/R_{side} ratio, is portrayed in Figure 4 where we plot this ratio versus k_T for both experiments at RHIC overlayed with theoretical predictions of a model that includes both a phase transition and a period of hadronic rescattering calculated with a microscopic transport code [18]. The model includes two scenarios with different critical temperatures and the authors note that a higher critical temperature leads to a longer period of rescattering in the hadronic phase. This in turn leads to a larger R_{out}/R_{side}ratio.

The data are completely inconsistent with this theoretical prediction, and with any physically reasonable hydrodynamic theoretical calculation to date. [17, 16]

3.2. Hydrodynamical Fits

The field of correlation measurements has adopted a method of interpretation based upon fits of the k_T dependence of the radii. The effect of Bose-Einstein correlations on a boost-invariant, hydrodynamically expanding source can be calculated analytically [19] to first order

$$R_{side}{}^2 = \frac{R_{geom}{}^2}{1+\beta_f^2(\frac{m_T}{T})} \tag{2}$$

where R_{geom} is the geometric radius of the source, $m_T^2 = k_T^2 + m_\pi^2$, β_f is the boost velocity ($\beta_T = \beta_f \frac{\rho}{R_{geom}}$) and T is the temperature. A fit of this functional form to the PHENIX data assuming T=125 MeV and $\beta_T = 0.69$ [4, 20] [4] is shown as a dashed line in Figure 4. The extracted radius is R_{geom} =6.7±0.2 fm.

Adding a second term in the expansion leads to the form [21]

$$R_{side}{}^2 = \frac{R_{geom}{}^2}{1+\eta_f^2(\frac{1}{2}+\frac{m_T}{T})} \tag{3}$$

in which η_f is the transverse rapidity boost $\eta_T = \eta_f \frac{\rho}{R_{geom}}$. The result of a fit to the PHENIX data with this form yields R_{geom} =8.1±0.3 fm. A fit of the STAR data to equation 3 yields R_{geom} =9.4±0.1 fm. These two fits are also shown in figure 4 All of these values for the geometric radius are much larger than the comparable 1D rms radius of the Au nucleus.

4. Conclusion

We have presented the first year measurements of identical pion correlations as a function of k_T by the PHENIX experiment at $\sqrt{s_{NN}}$=130 GeV. Comparisons to lower energies reveals a mild energy dependence in the longitudinal direction with no discernable transverse radius dependence. The ratio R_{out}/R_{side} is consistent with unity for all k_T in contrast to theoretical predictions that include a phase transition.

Acknowledgements

This work was performed under the auspices of the U.S. Department of Energy by the University of California, Lawrence Livermore National Laboratory under Contract No. W-7405-Eng-48.

References

1. G. Goldhaber, S. Goldhaber, W. Lee, and A. Pais, Phys. Rev. **120**, 200 (1960).
2. U. Wiedemann and U. Heinz, Phys. Rep. **319**, 145 (1999).
3. M.A. Lisa, U. Heinz, and U.A. Wiedemann Phys. Lett **B489** (2000) 287.
4. K. Adcox *et al.*, accepted for publication in Phys. Rev. Lett. nucl-ex/0201008.
5. D.P. Morrison, Nucl. Phys. **A638**, 565c (1998), N. Saito, *ibid*, 575c (1998).
6. K. Adcox *et al.* Phys. Rev. Lett. **86**, 3500 (2001).
7. M.D. Baker, Nucl. Phys. **A 610**, 213c (1996).
8. I.G. Bearden *et al.*, Phys. Rev. **C58**, 1656 (1998).

[4] These values are taken from fits to the singles spectra for the 5%-15% centrality bin.

9. M.M. Aggarwal *et al.*, Eur. Phys. Jour. **C16**, 445 (2000).
10. A.N. Makhlin and Y.M. Sinyukov, Z. Phys. **C39**, 69 (1988).
11. U. Wiedemann, P. Scotto, U. Heinz, Phys. Rev. **C 52**, 918 (1996).
12. R. Soltz, M.D. Baker, J.H. Lee, for the E802 Collaboration, Nucl. Phys. **A661**, 439 (1999), L. Ahle *et al.*, to be submitted to Phys. Rev. **C** (2002).
13. M. Lisa *et al.*, Phys. Rev. Lett. **84**, 2798 (2000).
14. K. Adcox *et al.* accepted for publication in Phys. Rev. Lett. (2002), nucl-ex/0201008.
15. C. Adler *et al.*, Phys. Rev. Lett. **87**, 082301 (2001).
16. U. Heinz in these proceedings.
17. D. Rischke and M. Gyulassy, Nucl. Phys. **A608**, 479 (1996).
18. S. Soff, S.A. Bass, and A. Dumitru, Phys. Rev. Lett. **86**, 3981 (2001).
19. S. Chapman, J.R. Nix, U. Heinz, Phys. Rev. **C52**, 2694 (1995).
20. K. Adcox *et al.*, to be submitted to Phys. Rev. C (2002).
21. U. Wiedemann, P. Scotto, U. Heinz, Phys. Rev. **C53**, 918 (1996).